

Regulation of synaptic timing in the olfactory bulb by an A-type potassium current

N. E. Schoppa and G. L. Westbrook

Vollum Institute, Oregon Health Sciences University, 3181 SW Sam Jackson Park Road, Portland, Oregon 97201, USA

Correspondence should be addressed to N.E.S. (schoppa@ohsu.edu)

Although rapid synaptic transmission confers signal fidelity, the activity of some neuronal circuits depends on prolonged excitation or inhibition. Here we demonstrate that GABAergic granule cells in the rat olfactory bulb produce prolonged inhibition of mitral cells through a precise kinetic matching between transmitter-gated and voltage-gated channels in their dendritic membrane. A transient A-type potassium current (I_A) specifically attenuated dendrodendritic inputs mediated by fast-acting AMPA receptors such that the excitation and subsequent inhibitory output of granule cells followed the prolonged kinetics of their NMDA receptors. Altering the weights of the AMPA and NMDA receptor-mediated inputs by modulating I_A provides a mechanism to regulate the timing of inhibition according to the demands on the bulb network.

The relay of information at most synapses in the central nervous system occurs rapidly, reflecting the fast activation and deactivation kinetics of postsynaptic ionotropic receptors, whereas slower neurotransmitter responses generally reflect the kinetics of second messenger-mediated signaling cascades. Exceptions to these rules exist, however. For example, the slow deactivation kinetics of NMDA receptors¹ can produce slow depolarizing responses and prolonged firing of action potentials²⁻⁴. Moreover, the high glutamate sensitivity of the NMDA receptor may cause 'pure' NMDA receptor-mediated synaptic responses following glutamate release at adjacent synapses⁵. GABA_A receptor-mediated inhibitory responses also can be prolonged because of slow recovery from desensitized states⁶. Whereas short-lasting synaptic responses are regarded as important for preserving signal fidelity, long-lasting synaptic responses may be critical for other functions in a neuronal circuit, for example, in the generation of oscillations and synchronous firing of neurons⁷.

Prolonged synaptic responses in the olfactory bulb are well characterized⁸⁻¹⁰. The stimulation of bulb mitral cells elicits a long-lasting excitatory response in GABAergic granule cells that in turn leads to long-lasting feedback inhibition of mitral cells at reciprocal dendrodendritic synapses. Both granule cell excitation and mitral cell inhibition rely on the activation of NMDA receptors^{11,12}. Because granule cells have both AMPA and NMDA receptors, the NMDA receptor dependence of granule cell activation presumably reflects a unique way of integrating synaptic inputs within their dendrites.

The impact of active dendritic conductances on the integration of synaptic inputs is recognized¹³⁻¹⁶. Thus, we examined the active properties of granule cells that might bias their excitation in favor of NMDA receptors. Using whole-cell patch-clamp recordings from olfactory bulb slices, we show that granule cells have a transient A-type potassium current (I_A) that allows throughput of prolonged NMDA receptor-mediated synaptic inputs, but not rapidly decaying AMPA receptor-mediated inputs.

The powerful role of I_A in discriminating synaptic inputs is not due to unusual types of receptors and channels in granule cells, but rather to the distribution of I_A channels, the granule cell morphology and the convergent mitral-to-granule cell anatomy within the bulb. The prolonged mitral cell inhibition that results from the interaction of I_A with synaptic inputs is likely to be critical for the generation of olfactory bulb oscillations and downstream processing of olfactory sensory information.

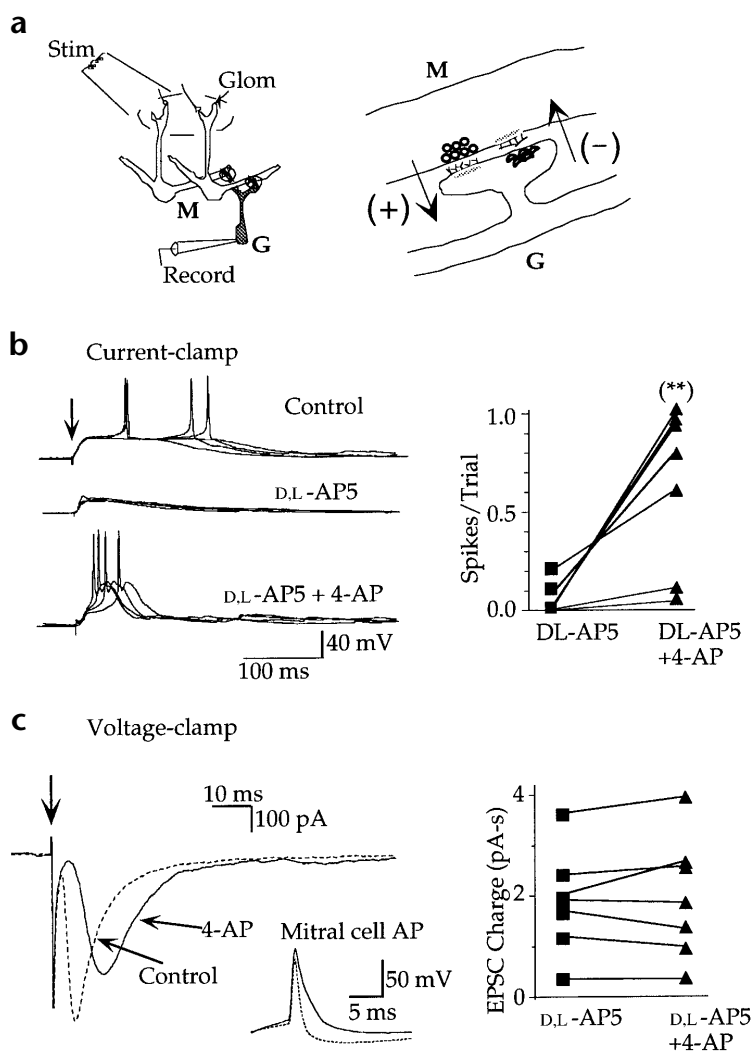
RESULTS

The excitatory response of granule cells is triggered by glutamate released at dendrodendritic synaptic contacts with secondary dendrites of mitral cells¹⁷. Mitral cells were stimulated via their primary dendrites by a bipolar stimulating electrode (100 V, 100 μ s) placed on a single glomerulus (Fig. 1a). As reported previously¹², glomerular stimulation elicited dual-component, AMPA and NMDA receptor-mediated voltage responses in granule cells (Fig. 1b), blocked by bath application of 1,2,3,4-tetrahydro-6-nitro-2,3-dioxobenzo[f]quinoxaline-7-sulfonamide (NBQX) and D,L-2-amino-5-phosphonopentanoic acid (D,L-AP5; $n = 5$). Dual-component responses also typically triggered the firing of action potentials. The number of evoked spikes was usually limited to one (1.12 ± 0.05 ; $n = 7$ cells), and the overall spiking frequency, including trials that failed to evoke spikes, was 0.51 ± 0.08 spikes per trial ($n = 20$). D,L-AP5 nearly abolished evoked spikes (0.04 ± 0.03 spikes per trial; $n = 7$), indicating that AMPA receptor-mediated synaptic inputs by themselves are ineffective in supporting granule cell excitation.

Rescue of excitation by blockade of I_A

We first tested if potassium conductances in granule cells were responsible for the limited efficacy of AMPA receptors. Following blockade of granule cell spiking with D,L-AP5, spiking remained low (0.032 ± 0.03 spikes per trial; $n = 5$) in tetraethylammonium (TEA; 10 mM), a non-specific antagonist of delayed-rectifi-

Fig. 1. Blockade of I_A with 4-AP enhances granule cell excitation by AMPA receptor-mediated synaptic inputs. **(a)** Morphology. The dominant component of inhibition in the olfactory bulb occurs at dendrodendritic synapses between the secondary dendrites of mitral cells (M) and the dendrites of granule cells (G). The cartoon on the right shows that glutamate released from the shaft of the mitral cell dendrite elicits excitation (+) of the granule spine, which in turn leads to recurrent GABAergic inhibition (-) of the activated mitral cell as well as lateral inhibition (-) of other mitral cells. **(b)** Glomerular stimulation (as shown in **a**) elicited spike firing in granule cells that was greatly reduced by D,L-AP5 (50 μ M), but then recovered with subsequent addition of 4-AP (6 mM). Four glomerular stimulation-evoked responses are shown from one cell for each condition on the left. The summary plot on the right reflects pooled data from responses elicited by glomerular stimulation (three cells) or by focal mitral cell stimulation (four cells). **(c)** The granule cell EPSC, as measured by its total charge (see Methods), was not increased in size by 4-AP, indicating that 4-AP did not enhance glutamate release from the mitral cell. The inset shows that 4-AP did broaden the mitral cell presynaptic action potential, accounting for the somewhat longer onset delay and duration of the EPSC in 4-AP. The summary on the right reflects the same experiments as in **(b)**.



er and calcium-activated types of potassium channels¹⁸. However, 4-aminopyridine (4-AP; 5–10 mM), an antagonist of transient A-type potassium channels (I_A) caused a dramatic recovery of spiking (0.66 ± 0.17 spikes per trial; $n = 7$; Fig. 1b). The rescue of granule cell excitation by 4-AP implies that I_A severely limits the effectiveness of AMPA receptor-mediated synaptic inputs. 4-AP can increase transmitter release by broadening the presynaptic action potential^{19,20}. Therefore, we tested whether the effect of 4-AP on granule cell excitation could be explained by enhanced glutamate release from mitral cells. To eliminate effects of 4-AP on the electrical responsiveness of mitral cells, we used a saturating stimulus intensity. 4-AP did broaden the mitral cell action potential (Fig. 1c, inset) but did not increase the granule cell EPSC ($3 \pm 7\%$ increase in the EPSC charge; $n = 7$) nor EPSPs at holding potentials below threshold for I_A (see Fig. 3c). Thus, the enhancement of granule cell firing by 4-AP reflects increased excitability of the postsynaptic granule cell membrane rather than a presynaptic effect on mitral cells.

Granule cells had a prominent transient I_A blocked by millimolar concentrations of 4-AP (Fig. 2a; $51 \pm 4\%$ block, 1 mM 4-AP, +12 mV; $n = 5$). I_A was unaffected by low concentrations of 4-AP (100 μ M; $n = 4$) or dendrotoxin (1 μ M; $n = 3$) and was only slightly reduced by TEA ($28 \pm 10\%$ block, 20 mM; $n = 4$). I_A measured in nucleated outside-out patches in the presence of TEA (10–20 mM; Fig. 2b) had a threshold activation voltage of -44 ± 2 mV ($n = 8$) and a midpoint voltage for steady-state inactivation of -66 ± 4 mV ($n = 5$). The activation threshold for I_A was near the threshold for granule cell spiking (-47 ± 2 mV; $n = 9$), indicating that I_A is capable of affecting spike initiation. I_A inactivated with a voltage-independent decay time constant (24 ± 5 ms at -38 mV; $n = 5$), and recovery from inactivation (at -108 mV) was approximated by a single exponential with $\tau = 62 \pm 10$ milliseconds ($n = 3$). Granule cells also had a delayed,

non-inactivating potassium current I_K blocked by TEA (10–20 mM; Fig. 2a) but not 4-AP ($6 \pm 4\%$ reduction in 5 mM 4-AP; $n = 4$). However, I_K had a threshold for activation (-33 ± 5 mV; $n = 5$) that was above the spike initiation voltage of granule cells, consistent with the lack of effect of TEA on spiking.

I_A specifically attenuates brief depolarizations

The attenuation of AMPA receptor-mediated synaptic inputs by I_A might be explained by the short duration of the AMPA receptor-mediated depolarization. Indeed, we found that granule cell depolarizations in response to short (2–4-ms) somatic current injections that mimicked an AMPA receptor-mediated EPSP (Fig. 3a) were significantly enhanced when I_A was blocked by 4-AP (by 7.2 ± 2.6 mV; $n = 5$). As expected, the effect of 4-AP depended on whether the injected current elicited a depolarization that reached the activation threshold for I_A . Longer somatic current injections (800 ms, +30 pA; Fig. 3b) elicited spiking in granule cells in the absence or presence of 4-AP, but 4-AP reduced the lag to spiking by 47 ± 15 milliseconds ($n = 6$). Close examination of the voltage traces showed that 4-AP enhanced the early portion of the responses, whereas all the responses converged to the same voltage at spike initiation, consistent with transient attenuation by I_A .

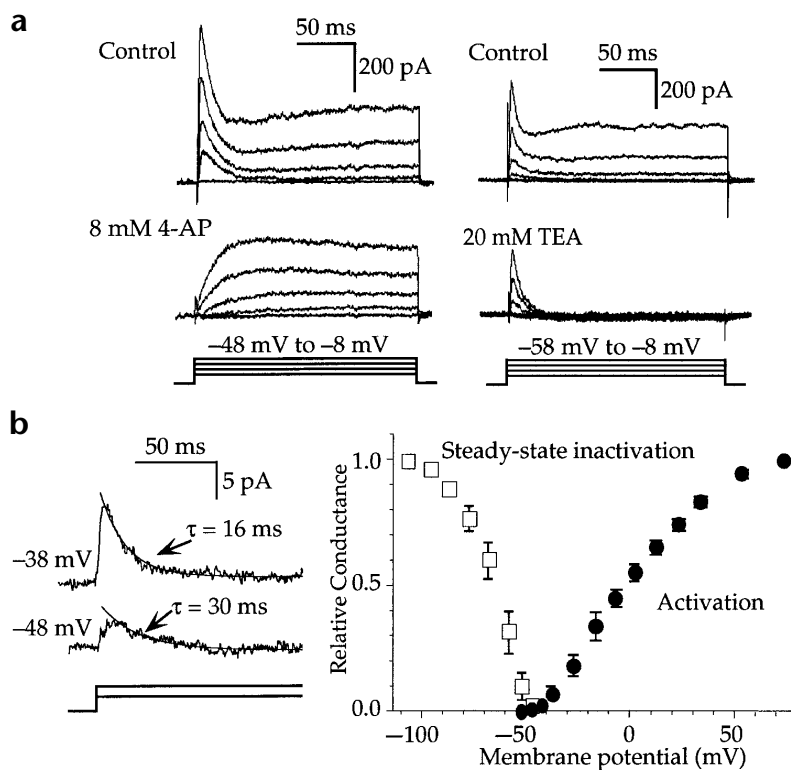


Fig. 2. Properties of I_A in granule cells. (a) Whole-cell potassium currents in granule cells had transient and steady-state components that were differentially sensitive to bath application of 4-AP (6 mM) and TEA (10 mM). Currents were induced by voltage pulses between -58 mV and -8 mV. (b) The transient current I_A measured in nucleated patches had an inactivation decay time constant near 20 ms. The threshold for activation of I_A in the patch experiments was near -45 mV, whereas the midpoint voltage for steady-state inactivation for I_A was near -65 mV. Each point in the activation and steady-state inactivation curves reflects 3–8 experiments. Steady-state inactivation was evaluated during a 40-ms test pulse (+2 mV), preceded by a 200-ms prepulse of varying amplitude.

As with somatic current injections, activation of AMPA receptor-mediated synaptic inputs (Fig. 3c) elicited EPSPs that were enhanced by 4-AP (by 6.4 ± 1.7 mV in 6 cells), whereas the single spike typically elicited by longer dual-component synaptic inputs occurred with a much shorter lag in 4-AP (Fig. 3d). Dual-component EPSPs under control conditions had a slowly rising depolarizing phase that was analogous to the upward creep (due to inactivation of I_A) observed in the control voltage responses to long somatic current injections. This slow phase produced a ~ 100 -millisecond delay to the peak of the EPSP (99 ± 18 ms; $n = 4$), as well as a pronounced delay (71 ± 11 ms; $n = 15$) and desynchrony in synaptically evoked spiking. Thus, the NMDA receptor-mediated depolarization in granule cells outlasts I_A , thereby eliciting spikes after a pronounced lag, whereas the AMPA receptor-mediated EPSP is counterbalanced by I_A .

Intrinsic membrane mechanisms in granule cells

The activation and inactivation properties of I_A in granule cells as described above were largely conventional¹⁸, as was the amplitude of the whole-cell I_A current ($I_{\text{peak}} = 1220 \pm 120$ pA, +2 mV; $n = 24$; see refs. 21, 22). We thus considered whether the localization of I_A could contribute to its powerful effect on the excitation of granule cells. Although the small diameter of the distal dendrites of granule cells precluded a direct measure of dendritic I_A channels, we made an indirect assessment by comparing whole-cell potassium currents with those in somatic patches (Fig. 4a and b). The ratio of the transient (I_A) to the steady-state component (I_K) of the whole-cell current ($I_A/I_K = 3.7 \pm 0.3$, $n = 25$) was much larger than in outside-out patches ($I_A/I_K = 1.0 \pm 0.2$, $n = 26$) or in cell-attached somatic patches ($I_A/I_K = 1.1 \pm 0.2$, $n = 4$). The whole-cell I_A and I_K ($n = 9$) had activation properties indistinguishable from the patch currents. Two cell-attached patches taken from proximal dendrites also showed a small transient component (Fig. 4b). The small tran-

sient current in patches suggests a relatively high density of I_A channels in distal dendrites of granule cells, where they would be in a good position to attenuate excitatory inputs.

The morphology of granule cells could also help explain the strong effect of I_A on spiking. Whereas action potentials in many neurons initiate in the axon hillock or initial segment²³, which contain high densities of sodium channels^{24,25}, spike initiation in the axonless granule cell must occur in the soma or dendrites. Sodium currents in somatic patches had typical properties, with an activation threshold of -41 ± 3 mV ($n = 7$), a steady-state inactivation midpoint voltage of -63 mV ($n = 2$) and rapid inactivation decay kinetics ($\tau = 0.90 \pm 0.11$ ms at -18 mV; $n = 8$). However, the maximum rate-of-rise of synaptically evoked somatic spikes in granule cells (116 ± 14 V per s; $n = 7$) was lower than in other cells (300 – 600 V per s; refs. 26, 27), consistent with a relatively low density of sodium channels.

I_A drives long-lasting inhibition of mitral cells

The unique mechanism by which I_A regulates the excitation of granule cells at dendrodendritic synapses would also be expected to affect the output of granule cells, that is, GABA release onto mitral cells. As observed for granule cell spiking, the GABA_A receptor-mediated IPSC in mitral cells is blocked by AP5, implying that GABA release depends on the activation of granule cell NMDA receptors^{11,12}. However, in the presence of 4-AP, IPSCs were only modestly reduced by AP5 (by $29 \pm 7\%$; $n = 5$), but completely blocked by subsequent addition of NBQX ($n = 5$; Fig. 5a), indicating that AMPA receptors can support GABA release when I_A is blocked (Fig. 5b). 4-AP also altered the kinetics of the IPSCs. In 11 mitral cells, 4-AP shortened the IPSC duration (Fig. 5c), reducing both its decay time constant (by $30 \pm 5\%$) and time to peak (from 60 ± 5 ms to 27 ± 2 ms). These kinetic changes were associated with an increased peak amplitude ($A_{4\text{-AP}}/A_{\text{Control}} = 1.53 \pm 0.12$; $n = 11$), although no change was detected in the IPSC charge ($Q_{4\text{-AP}}/Q_{\text{Control}} = 1.17 \pm 0.20$). 4-AP did not change the kinetics of the unitary synaptic events ($\tau_{\text{decay}} = 13 \pm 1$ and 13 ± 1 ms before and after 4-AP, respectively; $n = 5$), implying that the faster kinetics of the composite IPSC reflects disinhibition of the early AMPA receptor-mediated EPSP, leading to more synchronous GABA release. Thus, by controlling which receptor type elicits activation of granule cells, I_A effectively regulates the kinetics of mitral cell inhibition.

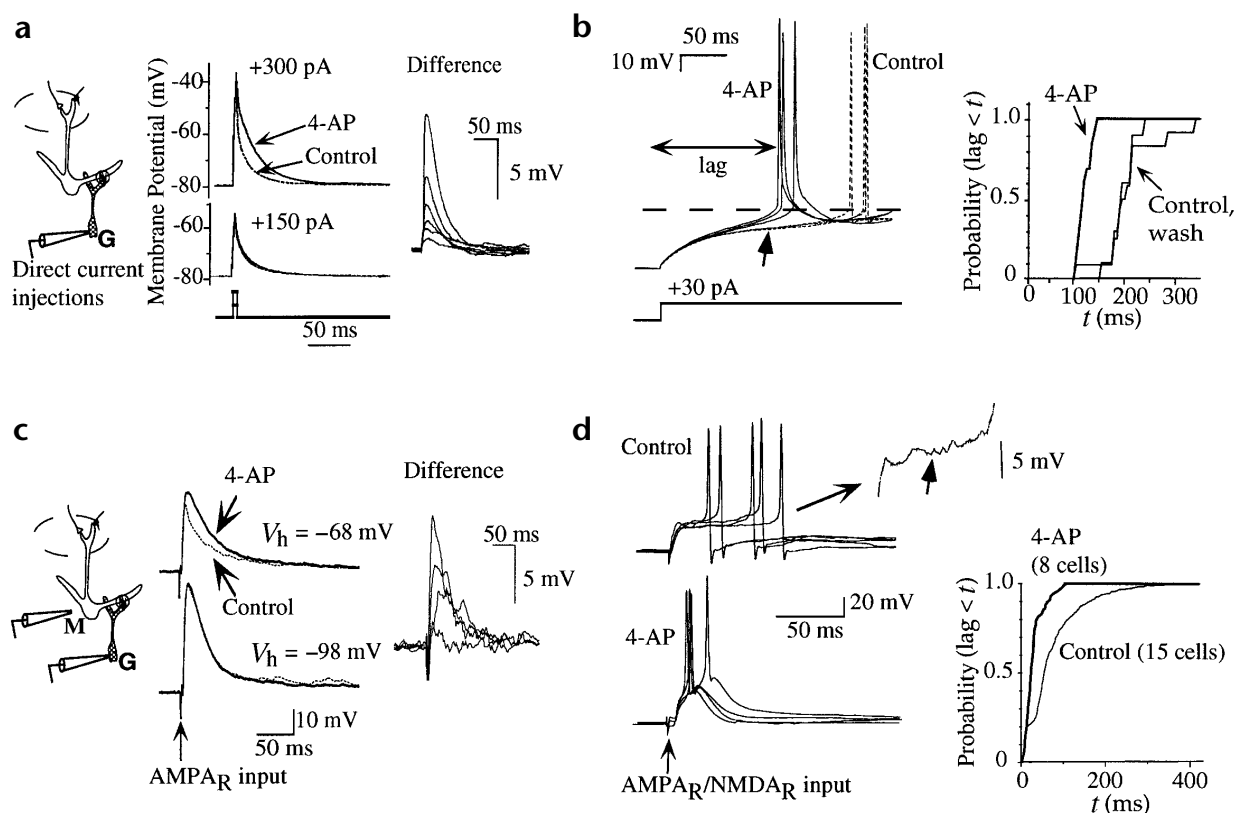


Fig. 3. I_A attenuates short but not prolonged current inputs. (a) Short-duration somatic current injections into a granule cell (2 ms, 150 to 300 pA) elicited depolarizations that were greatly enhanced when I_A was blocked by 4-AP. The magnitude of the 4-AP-effect ('Difference') was as much as 10 mV and depended on whether the depolarization reached I_A threshold. (b) Granule cell depolarizations in response to prolonged somatic current injections (800 ms, +30 pA) were transiently enhanced by 4-AP (arrow), but control responses eventually converged to the same amplitude as responses in 4-AP at spike threshold (dashed line). The difference in the lag to spiking in this experiment, plotted on the right as the cumulative probability of spiking, was between 50–100 ms. (c) 4-AP also enhanced short-duration AMPA receptor (AMPA_R)-mediated EPSPs in granule cells, measured in the presence of D,L-AP5 (50 μM). 4-AP enhanced EPSPs only when the depolarization reached I_A threshold (compare holding potentials, V_h , of -98 and -68 mV). EPSPs were evoked by focal mitral stimulation. (d) Prolonged $\text{AMPA}_R/\text{NMDA}_R$ -mediated synaptic responses in granule cells displayed an upward creep (inset, short arrow in inset), leading to spiking after a 4-AP-sensitive lag. The lag to spiking, used for construction of the histogram, was taken as the time between the stimulus and the peak of the evoked action potentials. Dual-component synaptic responses were evoked with glomerular stimulation.

Functions of I_A for reciprocal and lateral inhibition

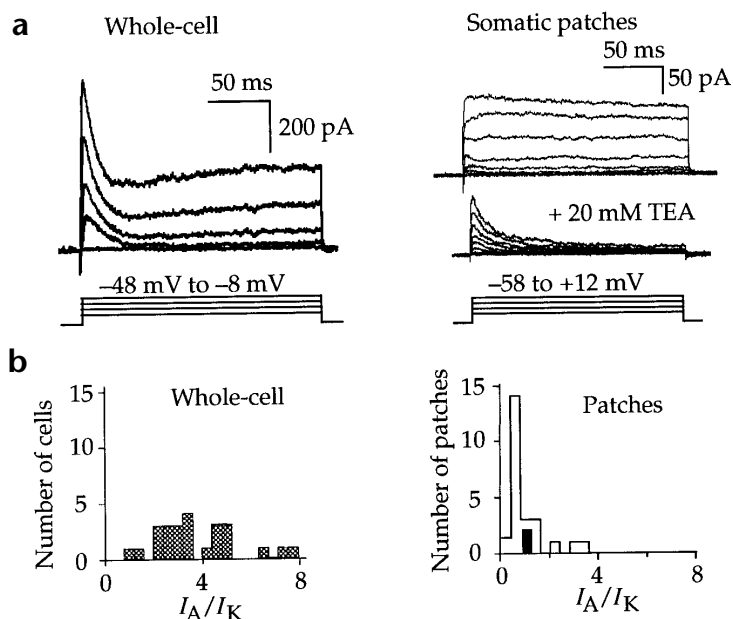
Glomerular stimulation-evoked dendrodendritic IPSCs have both a reciprocal component (as shown in Fig. 1a) and a lateral component reflecting inhibition between mitral cells through synaptically 'shared' granule cells. The mechanisms of generation of reciprocal and lateral inhibition may differ. For example, the spread of voltage in granule cells required for lateral inhibition is expected to be significantly augmented by action potentials, whereas reciprocal inhibition can be recorded in tetrodotoxin¹⁰, and thus requires only local signaling within dendritic spines. Similarly, reciprocal and lateral inhibition could be differentially regulated by I_A .

To isolate the lateral IPSC, we modified our standard glomerular stimulation protocol by including the sodium channel antagonist QX-314 (15 mM) in the patch pipet to block reciprocal inhibition (Fig. 6a). In 8 mitral cells, 4-AP did not affect the magnitude of the lateral IPSC ($Q_{4\text{-AP}}/Q_{\text{Control}} = 1.09 \pm 0.15$), but reduced its decay time constant by $20 \pm 6\%$ and time to peak from 60 ± 8 to 38 ± 4 ms (Fig. 6b). The kinetic effects of 4-AP on the lateral IPSC were presumably due to the shortened latency to synaptically evoked spiking in granule cells (Fig. 3d). Indeed, a direct comparison between the predicted IPSC based on the

timing of granule cell spiking and the observed lateral IPSC (Fig. 6b) showed a close match in the time to peak for the predicted and observed IPSCs, consistent with a 4-AP-induced change in triggering of the lateral IPSC. The observed IPSCs were longer in duration than predicted, perhaps reflecting GABA release driven by a spike-induced residual calcium signal²⁸.

The reciprocal IPSC was isolated by direct stimulation (2–4 ms voltage steps to 0 mV) of a mitral cell (Fig. 6c). We first performed experiments in reduced extracellular magnesium to enhance the amplitude of the reciprocal IPSC¹². In 100 μM Mg^{2+} , 4-AP markedly changed the kinetics of the reciprocal IPSC from a slow monophasic decay ($\tau = 478 \pm 28$ ms; $n = 8$) to a biphasic decay with fast and slow components ($\tau_f = 59 \pm 11$ ms, $\tau_s = 528 \pm 49$ ms, $A_f/A_s = 2.5 \pm 0.6$). 4-AP increased the total charge associated with the reciprocal IPSC ($Q_{4\text{-AP}}/Q_{\text{Control}} = 2.1 \pm 0.3$) by introducing a fast component, as well as by causing a modest 1.4 ± 0.2 -fold increase in the slow component. A large rapid component was also induced by 4-AP in IPSCs measured in our standard extracellular solution containing 1 mM Mg^{2+} ($\tau = 32 \pm 7$ ms; $n = 8$; Fig. 6d). Quantitative analysis of the slow component of these reciprocal

Fig. 4. I_A channels in granule cells are localized in dendrites. (a) Potassium currents recorded in the whole-cell configuration had a much larger transient component (I_A) compared with currents in nucleated patches from the soma. Indeed, somatic patch currents showed no obvious I_A until the steady-state component (I_K) was blocked with TEA. (b) Histograms plotting the ratio I_A/I_K in whole-cell and somatic patches show that the relative amplitude of the whole-cell I_A was several times larger than in the soma, consistent with a high density of I_A channels in the distal dendrites of granule cells. The whole-cell and somatic-patch histograms reflect 25 and 26 measurements, respectively. Ratios were derived from currents measured at +2 mV. The solid bar in the patch histogram reflects two cell-attached patch measurements in the proximal dendrite (<15 μ m from the soma).



IPSCs, however, was precluded by the heightened level of baseline synaptic noise in 4-AP.

A 4-AP-induced rapid component in the IPSC ($\tau = 38 \pm 15$ ms; $n = 3$) was also observed in the presence of tetrodotoxin (1 μ M), confirming that the mechanism by which I_A affects reciprocal inhibition occurs locally, at dendritic spines on granule cells. The rapid IPSC was insensitive to D,L-AP5 (50 μ M; $n = 3$) but blocked by NBQX (10 μ M; $n = 2$), indicating that it reflects the enhanced AMPA receptor-mediated EPSP (Fig. 3c). Dual-component EPSPs were also enhanced by 4-AP (by 4.4 ± 1.6 mV and 3.5 ± 1.5 mV at 30 and 200 ms after the stimulus, respectively), consistent with the enlarged rapid and slow components of the reciprocal IPSC (100 μ M Mg^{2+}).

DISCUSSION

Synaptic transmission at dendrodendritic synapses between mitral cells and granule cells in the olfactory bulb is characterized by its slow kinetics and unusual dependence on the activation of NMDA receptors. We found that 4-AP, a blocker of transient A-type potassium channels, I_A , rescued the efficacy of AMPA receptors in supporting synaptically evoked spiking in granule cells, indicating that I_A functions as a powerful regulator of AMPA and NMDA receptor-mediated inputs. Blockade of I_A also fundamentally changed the characteristics of inhibition in the olfactory bulb circuit, from a kinetically slow process mediated by NMDA receptors to a more rapid process mediated largely by AMPA receptors.

An I_A -mediated synaptic switch on excitability

4-AP is known to affect a number of potassium currents¹⁸ and has both pre- and postsynaptic actions on the excitability of neurons. In granule cells, however, the effect of 4-AP was limited to a transient potassium current with the kinetic and pharmacological properties of I_A , whereas low concentrations of 4-AP that block I_D ²⁹ had no effect. The rapid kinetics of recovery from inactivation of I_A in granule cells are consistent with the properties of the Kv4.2 potassium channel³⁰, which is highly expressed in olfactory bulb granule cells³¹. Fortuitously for our analysis, 4-AP enhanced the excitatory responses of granule cells without increasing glutamate release from mitral cells (see also refs. 32, 33). The negligible effect of 4-AP on glutamate release may be due to saturation of the calcium sensor in the release machinery in the mitral cell secondary dendrites or to rapid calcium diffusion in the large-diameter mitral cell dendritic shaft.

Although I_A has been shown to affect excitability and synaptic integration in other neurons^{15,34,35}, the distinctive feature of I_A -mediated attenuation of granule cell excitability is that it discriminates between synaptic inputs on the basis of their durations. By keeping the granule cell membrane potential below spike threshold, I_A prevents spike initiation by short-duration AMPA receptor-mediated inputs. I_A also exerts a local effect on voltage transients in granule cell spines under weaker stimulus conditions, because AMPA receptors are largely ineffective in supporting local depolarization-driven reciprocal inhibition^{11,12} unless I_A channels are blocked. By mediating depolarization that acts to relieve magnesium block from granule cell NMDA receptors^{11,12}, AMPA receptors on granule cells do have an important facilitatory function within the dendrodendritic circuitry. However, AMPA receptor activation alone is insufficient to initiate spikes or local depolarization-driven GABA release in granule cells.

Paradoxically, 4-AP changed the glutamate receptor dependence of the glomerular stimulation-evoked IPSC without causing a detectable change in its total charge, implying that blockade of I_A not only enhances the AMPA receptor-mediated drive onto granule cells but also reduces GABA release mediated by NMDA receptors. The reduced NMDA receptor-mediated drive for lateral inhibition can be explained by the spike firing pattern in granule cells (Figs. 1b and 3d). Spike-activated potassium conductances elicit a hyperpolarization or shunt that generally limits a synaptic response to a single action potential, such that early AMPA receptor-mediated spiking in 4-AP inhibits late spiking driven by the NMDA receptor-mediated EPSP. 4-AP did cause a net increase in the magnitude of local depolarization-driven GABA release. However, because the reciprocal IPSC made only a small contribution to the glomerular stimulation-evoked IPSC, the increase in the reciprocal component was not detectable in these measurements.

Integration in granule cell dendrites

I_A is well known for its effects on repetitive spiking. The prominent role for the granule cell I_A in synaptic integration does not seem to be due to a uniformly high density of I_A channels or unusual activation properties. The steady-state inactivation properties of I_A in granule cells are, however, rather atypical. Where-

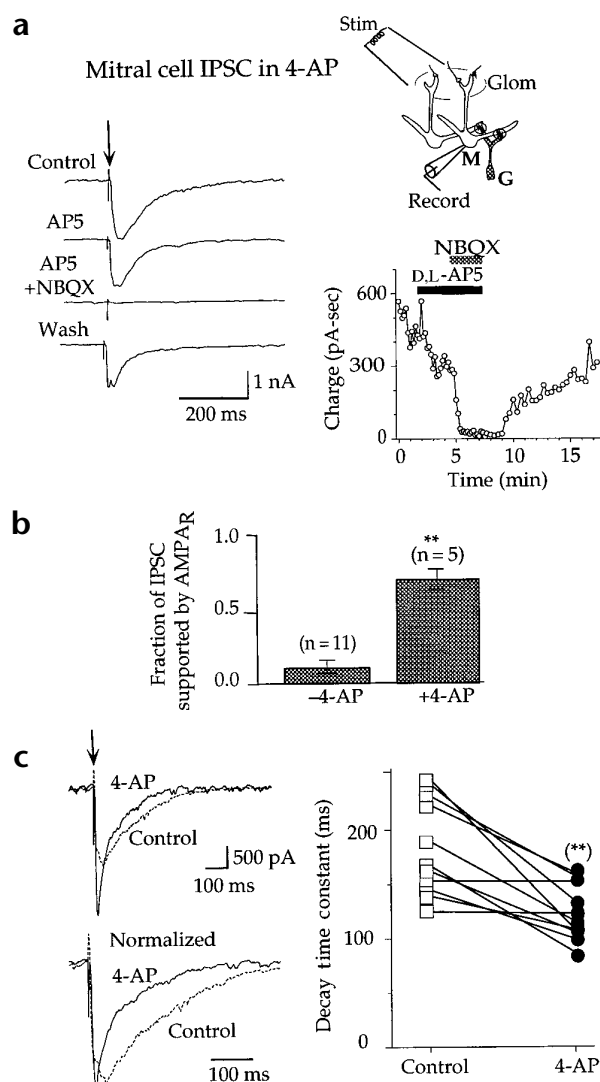


Fig. 5. Blockade of I_A elicits rapid, AMPA receptor-driven mitral cell inhibition. (a) In the continuous presence of 4-AP (6 mM), IPSCs evoked in mitral cells by glomerular stimulation were only slightly reduced by D,L-AP5 (50 μ M), but were completely blocked by subsequent addition of NBQX (5 μ M). (b) The fraction of the IPSC supported by AMPA receptors, as estimated from the AP5-induced reduction in IPSC charge, averaged 70% in the presence of 4-AP, as compared with only 14% under control conditions. (c) 4-AP accelerated the kinetics of IPSCs measured in response to the dual-component synaptic input, which was most apparent when the currents were normalized (lower trace). 4-AP reduced the time-to-peak of the IPSC as well as the decay time constant, as shown for 11 cells on the right.

as in many neurons I_A is nearly completely inactivated at the resting potential^{18,36}, I_A in granule cells is only half-inactivated at rest (-66 mV), making a large fraction of I_A channels available to affect synaptic inputs. I_A channels in granule cells also appear to have higher expression in dendrites. A preferential dendritic localization of I_A has been shown in other neurons^{15,37}, but I_A channels may have a particularly robust effect on spiking in granule cells, owing to their high input resistance (~ 1 G Ω)¹², their axonless morphology and a low density of sodium channels.

The function of I_A in discriminating synaptic inputs based on their duration relies also on the nature of the incoming synaptic traffic within the olfactory bulb. In many neurons, voltage-dependent magnesium block greatly reduces NMDA receptor-mediated responses^{38,39}, thus limiting the magnitude of any prolonged depolarization that would be available to outlast I_A . However, the convergent mitral–granule cell connectivity in the bulb generates a large glomerular stimulation-evoked depolarization in single granule cells that overcomes magnesium block of NMDA receptors. NMDA receptors in granule cells have a typically high sensitivity to magnesium¹², emphasizing that granule cells have an I_A -mediated mechanism to regulate their excitability while having receptors and voltage-gated channels with typical intrinsic properties.

Timing of inhibition in the olfactory bulb

Blockade of I_A with 4-AP reduced the onset time and accelerated the decay kinetics of mitral cell inhibition, reflecting the faster AMPA receptor-mediated drive onto granule cells. The more rapid inhibition was in part due to a reduction in the latency to spike firing in granule cells, as well as enhanced GABA release driven by local, AMPA receptor-mediated depolarizations in the granule cell spine. The faster inhibition in 4-AP implies that I_A functions in the olfactory bulb circuit to generate inhibition following prolonged NMDA receptor activation. Such long-lasting reciprocal inhibition (~ 200 ms) might be required for appropriate downstream coding of odorant information carried by single mitral cells, whereas prolonged lateral inhibition would inhibit the delayed spiking that occurs in other mitral cells in response to an odorant⁴⁰. Prolonged inhibition is also proposed as a general requirement for circuits whose functions rely on oscillations and neuronal synchronization⁷, as in the case of olfactory sensory information processing in some systems^{41,42}.

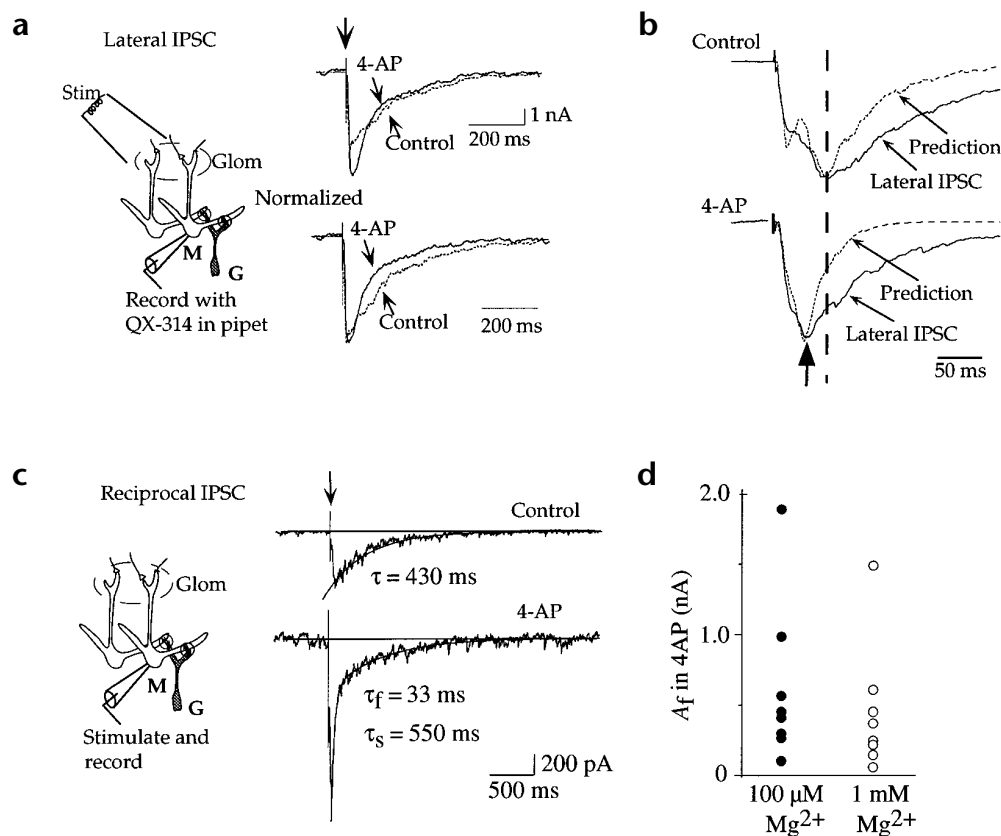
The I_A -mediated mechanism for generating slow inhibition is also advantageous, as it allows for dynamic regulation. Modulation of I_A could occur through the action of protein kinases and intracellular calcium^{43–46} or through changes in the granule cell membrane voltage. Inactivation of I_A in response to a previous depolarizing input would produce inhibition with shortened kinetics but with a larger peak amplitude. Such inhibition might be most effective against a rapid train of action potentials occurring in response to high concentrations of odor⁴⁷. By controlling the relative effectiveness of the AMPA and NMDA receptor-mediated synaptic inputs, regulation of I_A allows fine-tuning of inhibition according to the demands on the bulb network.

METHODS

Horizontal slices (400 μ m) were prepared from olfactory bulbs taken from 10–23 day-old Sprague-Dawley rats, as described¹², and viewed under DIC optics (Axioskop, Carl Zeiss). All experiments were done at room temperature (20–24°C).

Measurement of synaptic responses. Synaptic responses were recorded using a base extracellular bath solution that contained 125 mM NaCl, 25 mM NaHCO₃, 1.25 mM NaH₂PO₄, 25 mM glucose, 2.5 mM KCl, 2 mM CaCl₂ and 1 mM MgCl₂ at pH 7.3 and was oxygenated with 95% O₂/5% CO₂. Granule cell EPSPs and EPSCs were recorded with picrotoxin (50 μ M) added to the bath and with patch pipets (8–13 M Ω) that contained 125 mM potassium gluconate, 2 mM MgCl₂, 2 mM CaCl₂, 10 mM EGTA, 2 mM Na-ATP, 0.5 mM Na-GTP and 10 mM HEPES, adjusted to pH 7.3 with KOH. Mitral cell IPSCs were recorded using pipets (1–3 M Ω) with equimolar replacement of potassium gluconate with KCl. Voltage-clamp recordings were done using series-resistance compensation (60–90%) at a holding potential between -70 and -80 mV. Data acqui-

Fig. 6. I_A regulates the kinetics of lateral and reciprocal inhibition. (a) The lateral IPSC was evoked with glomerular stimulation in the presence of QX-314 (15 mM) in the recording pipet. Blocking I_A with 4-AP caused a modest acceleration in the decay of the lateral IPSC. (b) On an expanded time scale, it can be seen that 4-AP also reduced the time-to-peak of the lateral IPSC (compare vertical dashed line with thick arrow at bottom). The displayed lateral IPSCs reflect averages from five cells. The dotted curves are the predicted time courses of the lateral IPSCs, derived from the timing of spike firing in granule cells. The close match in the time to peak of the predicted and measured currents is consistent with spike-mediated triggering of the lateral IPSC. The predicted IPSC reflects the convolution of the probability-density function for the spiking lag in granule cells (Fig. 3d) with the time course of the spontaneously occurring IPSC in mitral cells (sum of two exponentials, $\tau_{\text{rise}} = 0.5$ ms and $\tau_{\text{decay}} = 20$ ms). (c) The reciprocal IPSC, elicited by direct depolarization of the test mitral cell (2 ms, 0 mV), was slowly decaying under control conditions, but 4-AP introduced a pronounced rapid component (τ_r). The reciprocal IPSC was augmented by using a reduced concentration (100 μM) of extracellular magnesium. (d) The 4-AP-induced rapid IPSC had a large amplitude (A_f) in both 100 μM and 1 mM Mg^{2+} . An estimate of A_f in 100 μM Mg^{2+} was obtained from double-exponential fits of the IPSCs (as in c). For measurements done in 1 mM Mg^{2+} , A_f was taken as the peak of the 4-AP-induced rapidly decaying IPSC.



sition was terminated when the access resistance was greater than 15 M Ω . Except where noted, current-clamp recordings were made while holding granule cells near their resting potentials (-66 ± 2 mV; $n = 32$). Single visualized glomeruli were stimulated with a bipolar tungsten electrode (tip separation, 125 μm ; World Precision Instruments, Sarasota, FL). We used maximal stimulation (100 V, 100 μs duration), which generally elicited maximum-amplitude responses. For focal mitral cell stimulation, a 2–3 M Ω patch pipet filled with extracellular solution was positioned above the soma of a mitral cell within 150 μm of the recorded granule cell. In recordings of reciprocal IPSCs, sodium and potassium currents evoked by the depolarizing pulse, as estimated from the current remaining in bicuculline (50 μM), were subtracted. Current and voltage signals recorded with an Axopatch 200A amplifier (Axon Instruments, Foster City, California) were filtered at 1–5 kHz using an eight-pole Bessel filter and digitized at 2–10 kHz. Data were acquired on an IBM 486 clone using PCLAMP version 6, and were analyzed with AXOGRAPH (Axon Instruments). Synaptic charge transfer was estimated by numerically integrating the baseline-subtracted current during a 30–50-ms window for EPSCs and 500–1500-ms window for IPSCs. Statistical significance ($p < 0.05$), denoted by double asterisks, was determined using the Student's t -test. Except where noted, each of the displayed traces reflects an average of at least eight responses.

Measurement of potassium and sodium currents. Whole-cell and outside-out patch recordings of granule cell potassium currents were made with D,L-AP5 (50 μM), CNQX (10 μM) and tetrodotoxin (1 μM) added to the bath. TEA (10–20 mM), added to the bath for characterizing patch I_A , caused a modest block of I_A , but had no apparent effect on the activation

of unblocked I_A channels ($n = 5$). A reduced concentration (0.1 mM) of EGTA in the pipet solution or Cd (100 μM) in the bath were used in some recordings, but these modifications had no effect on I_A activation. Cell-attached recordings of I_A , done with equimolar replacement of the pipet potassium gluconate with NaCl, were made during +80 to +120 mV voltage steps. Measurements of sodium currents in outside-out patches were made with 50 μM picrotoxin, 50 μM D,L-AP5, 10 μM CNQX, 200 μM Cd, 20 mM TEA and 5 mM 4-AP added to the bath. The holding potential was -78 mV. The leak current was subtracted using a P/4 protocol. Measurements of I_A amplitude in Fig. 4b were made by isolating I_A with TEA (10–20 mM) or, alternatively, from the current measured at 1.5 ms, the time point at which I_A peaked in the isolated currents.

ACKNOWLEDGEMENTS

This work was supported by National Institute of Health grants 5F32 DC00270 to NES and NS26494 to GLW. We thank John Adelman for helpful comments on the manuscript.

RECEIVED 20 AUGUST; ACCEPTED 12 OCTOBER 1999

- Lester, R. A., Clements, J. D., Westbrook, G. L. & Jahr, C. E. Channel kinetics determine the time course of NMDA receptor-mediated synaptic currents. *Nature* 346, 565–567 (1990).
- Salt, T. E. Mediation of thalamic sensory input by both NMDA receptors and non-NMDA receptors. *Nature* 322, 263–265 (1986).
- Dickenson, A. H. & Sullivan, A. F. Differential effects of excitatory amino acid antagonists on dorsal horn nociceptive neurones in the rat. *Brain Res.* 506, 31–39 (1990).

4. D'Angelo, E., De Filippi, G., Rossi, P. & Taglietti, V. Synaptic excitation of individual rat cerebellar granule cells in situ: evidence for the role of NMDA receptors. *J. Physiol. (Lond.)* **484**, 397–413 (1995).
5. Kullmann, D. M. & Asztely, F. Extrasynaptic glutamate spillover in the hippocampus: evidence and implications. *Trends Neurosci.* **21**, 8–14 (1998).
6. Jones, M. V. & Westbrook, G. L. Desensitized states prolong GABA_A channel responses to brief agonist pulses. *Neuron* **15**, 181–191 (1995).
7. Buzsáki, G. Functions for interneuronal nets in the hippocampus. *Can. J. Physiol. Pharmacol.* **75**, 505–515 (1997).
8. Mori, K. & Takagi, S. F. An intracellular study of dendrodendritic inhibitory synapses on mitral cells in the rabbit olfactory bulb. *J. Physiol. (Lond.)* **279**, 569–588 (1978).
9. Nowycky, M. C., Mori, K. & Shepherd, G. M. GABAergic mechanisms of dendrodendritic synapses in isolated turtle olfactory bulb. *J. Neurophysiol.* **46**, 639–648 (1981).
10. Jahr, C. E. & Nicoll, R. A. An intracellular analysis of dendrodendritic inhibition in the turtle in vitro olfactory bulb. *J. Physiol. (Lond.)* **326**, 213–234 (1982).
11. Isaacson, J. S. & Strowbridge, B. W. Olfactory reciprocal synapses; dendritic signaling in the CNS. *Neuron* **20**, 749–761 (1998).
12. Schoppa, N. E., Kinzie, J. M., Sahara, Y., Segerson, T. P. & Westbrook, G. L. Dendrodendritic inhibition in the olfactory bulb is driven by NMDA receptors. *J. Neurosci.* **18**, 6790–6802 (1998).
13. Johnston, D., Magee, J. C., Colbert, C. M. & Cristie, B. R. Active properties of neuronal dendrites. *Annu. Rev. Neurosci.* **19**, 165–86 (1996).
14. Yuste, R. & Tank, D. W. Dendritic integration in mammalian neurons, a century after Cajal. *Neuron* **16**, 701–716 (1996).
15. Hoffman, D. A., Magee, J. C., Colbert, C. M. & Johnston, D. K⁺ channel regulation of signal propagation in dendrites of hippocampal pyramidal neurons. *Nature* **387**, 869–875 (1997).
16. Magee, J. C. Dendritic hyperpolarization-activated currents modify the integrative properties of hippocampal CA1 pyramidal neurons. *J. Neurosci.* **18**, 7613–7624 (1998).
17. Rall, W., Shepherd, G. M., Reese, T. S. & Brightman, M. W. Dendrodendritic synaptic pathway for inhibition in the olfactory bulb. *Exp. Neurol.* **14**, 44–56 (1966).
18. Rudy, B. Diversity and ubiquity of K channels. *Neuroscience* **25**, 729–749 (1988).
19. Molgo, J., Lemeignan, M. & Lechat, P. Effects of 4-aminopyridine at the frog neuromuscular junction. *J. Pharm. Exp. Ther.* **202**, 653–663 (1977).
20. Lundh, H. Effects of 4-aminopyridine on neuromuscular transmission. *Brain Res.* **153**, 307–318 (1978).
21. Huguenard, J. R., Coulter, D. A. & Prince, D. A. A fast transient potassium current in thalamic relay neurons: kinetics of activation and inactivation. *J. Neurophysiol.* **66**, 1304–1315 (1991).
22. Bardoni, R. & Belluzzi, O. Kinetic study and numerical reconstruction of A-type current in granule cells of rat cerebellar slices. *J. Neurophysiol.* **69**, 2222–2231 (1993).
23. Coombs, J. S., Curtis, D. R. & Eccles, J. C. The interpretation of spike potentials of motoneurons. *J. Physiol. (Lond.)* **139**, 198–231 (1955).
24. Wollner, D. & Catterall, W. A. Localization of sodium channels in axon hillocks and initial segments of retinal ganglion cells. *Proc. Natl. Acad. Sci. USA* **83**, 8424–8428 (1986).
25. Angelides, K. J., Elmer, L. W., Loftus, D. & Elson, E. Distribution and lateral mobility of voltage-dependent sodium channels in neurons. *J. Cell Biol.* **106**, 1911–1925 (1988).
26. Azouz, R., Jensen, M. S. & Yaari, Y. Ionic basis of spike after-depolarization and burst generation in adult rat hippocampal CA1 pyramidal cells. *J. Physiol. (Lond.)* **492**, 211–223 (1996).
27. Stuart, G., Schiller, J. & Sakmann, B. Action potential initiation and propagation in rat neocortical pyramidal neurons. *J. Physiol. (Lond.)* **505**, 617–632 (1997).
28. Goda, Y. & Stevens, C. F. Two components of transmitter release at a central synapse. *Proc. Natl. Acad. Sci. USA* **91**, 12942–12946 (1994).
29. Storm, J. F. Temporal integration by a slowly inactivating K⁺ current in hippocampal neurons. *Nature* **336**, 379–381 (1988).
30. Petersen, K. R. & Nerbonne, J. M. Expression environment determines K⁺ current properties: Kv1 and Kv4 alpha-subunit-induced K⁺ currents in mammalian cell lines and cardiac myocytes. *Pflügers Arch.* **437**, 381–392 (1999).
31. Serodio, P. & Rudy, B. Differential expression of Kv4 K⁺ channel subunits mediating subthreshold transient K⁺ (A-type) currents in rat brain. *J. Neurophysiol.* **79**, 1081–1091 (1998).
32. Muller, D. Potentiation by 4-aminopyridine of quantal acetylcholine release at the Torpedo nerve-electroplaque junction. *J. Physiol. (Lond.)* **379**, 479–493 (1986).
33. Spencer, A. N., Przysiecki, J., Acosta-Urquidí, J. & Basarky, T. A. Presynaptic spike broadening reduces junctional potential amplitude. *Nature* **340**, 636–638 (1989).
34. Segal, M., Rogawski, M. A. & Barker, J. L. A transient potassium conductance regulates the excitability of cultured hippocampal and spinal neurons. *J. Neurosci.* **4**, 604–609 (1984).
35. Cassell, J. F. & McLachlan, E. M. The effect of a transient outward current (I_A) on synaptic potentials in sympathetic ganglion cells of the guinea-pig. *J. Physiol. (Lond.)* **374**, 273–288 (1986).
36. Connor, J. A. & Stevens, C. F. Voltage clamp studies of a transient outward membrane current in gastropod neural somata. *J. Physiol. (Lond.)* **213**, 21–30 (1971).
37. Sheng, M., Tsaur, M.-L., Jan, Y. N. & Jan, L. Y. Subcellular segregation of two A-type K⁺ channel proteins in rat central neurons. *Neuron* **9**, 271–284 (1992).
38. Mayer, M. L., Westbrook, G. L. & Guthrie, P. B. Voltage-dependent block by Mg²⁺ of NMDA responses in spinal cord neurones. *Nature* **309**, 261–263 (1984).
39. Nowak, L., Bregestovski, P., Ascher, P., Herbet, A. & Prochiantz, A. Magnesium gates glutamate-activated channels in mouse central neurones. *Nature* **307**, 462–465 (1984).
40. Hamilton, K. A. & Kauer, J. S. Patterns of intracellular potentials in salamander mitral/tufted cells in response to odor stimulation. *J. Neurophysiol.* **62**, 609–625 (1989).
41. Tank, D. W., Gelperin, A. & Kleinfeld, D. Odors, oscillations, and waves: does it all compute? *Science* **265**, 1819–1820 (1994).
42. Stopfer, M., Bhagavan, S., Smith, B. H. & Laurent, G. Impaired odour discrimination on desynchronization of odour-encoding neural assemblies. *Nature* **390**, 70–74 (1997).
43. Chen, Q. X. & Wong, R. K. Intracellular Ca²⁺ suppressed a transient potassium current in hippocampal neurons. *J. Neurosci.* **11**, 337–343 (1991).
44. Gage, P. W. Activation and modulation of neuronal K⁺ channels by GABA. *Trends Neurosci.* **15**, 46–51 (1992).
45. Covarrubias, M., Wei, A., Salkoff, L. & Vyas, T. B. Elimination of rapid potassium channel inactivation by phosphorylation of the inactivation gate. *Neuron* **13**, 1403–1412 (1994).
46. Hoffman, D. A. & Johnston, D. Downregulation of transient K⁺ channels in dendrites of hippocampal CA1 pyramidal neurons by activation of PKA and PKC. *J. Neurosci.* **18**, 3521–3528 (1998).
47. Harrison, T. A. & Scott, J. W. Olfactory bulb responses to odor stimulation: analysis of response pattern and intensity relationships. *J. Neurophysiol.* **56**, 1571–1589 (1986).